

**NEW CONCEPT FOR WIND TURBINE TESTING RIG**

Friedrich Klinger, Zhong Chen  
 INNOWIND Forschungsgesellschaft mbH  
 Altenkesslerstr. 17/D2, 66115 Saarbrücken, Germany

**Summary**

Wind turbines are exposed to fatigue loads during their life time of 20 years. They have to bear up to  $10^9$  load cycles. Therefore the durability prediction is very important. Pure computer simulation can no longer fulfil this requirement, so that real fatigue testing on a testing rig is moved now more and more to the foreground.

Existing testing equipment is mostly cost-intensive, because the reproduction of the wind loads has to be applied by hydraulic drives with high frequencies and very high power input.

INNOWIND has developed a new concept for a testing rig for the drive train including nacelle and rotor hub. This testing rig will be operated at very low power input and will perform both the electrical and mechanical testing.

The data and the model used in this presentation are based on a wind turbine with 2.5 MW rated power and 103 m rotor diameter.

**1. Requirement**

Electrical failure leads mostly to down time in power production, but mechanical failure could cause total turbine loss and even peoples lives. Testing rig for wind turbines should be able to test power electronics and mechanical components by extreme- and fatigue loading. In addition, the testing rig should fulfil the following requirements:

- a) On the new testing rig the drive train should include the hub, the blade bearings, the pitch drives and rotor blades near the hub area in addition to the loads from the gearbox, generator, frame and azimuth bearing.
- b) The testing rig should be operated at high frequency loads and low energy input compared to existing test equipments.
- c) The investment costs of the testing rig should be lower than today, so that the turbine manufacturer will be able to perform tests on their own equipment. Testing institutes might assist in planning, operating and interpreting the testing results.
- d) It would be best, if the testing could be run in the open air, no building will be needed. Up to now testing rigs have been installed in extremely expensive buildings.
- e) The loads on the foundation should be much lower than on conventional testing rigs.

**2. Concept**

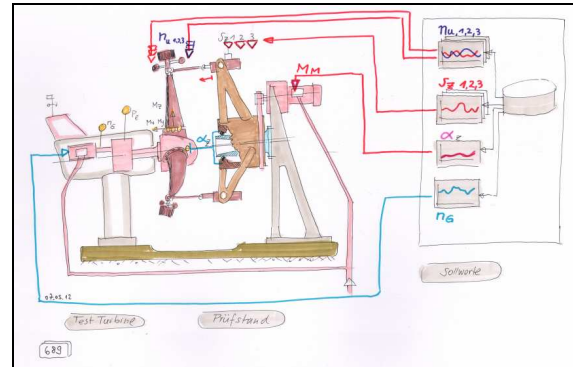
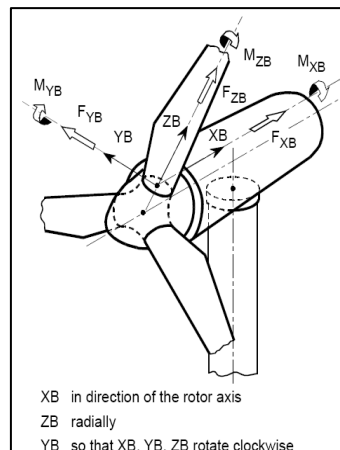


fig 1 test strategy for INNOWIND new concept

The fig 1 shows the INNOWIND concept. Instead of applying loads at the end of the main shaft as the conventional testing rigs do, the load introduction takes place directly on the blades in a distance L from the hub. So the blade bearings, the pitch drives, the rotor blade near the hub area and the hub are included in the drive train and are subject to the fatigue testing. Fatigue loading of the hub and of the blade bearings is getting more and more important for Multi Megawatt Turbines as bending loads and stress at the blade root are influenced up to 90 % only by the weight of the blades. It is an important feature of this new concept, that these bending loads, influenced by gravity, are reproduced in the hub by rotating masses with no extra power input.

According to fig 4, analysing time histories for blade root loads  $M_y$  and  $F_x$  during power production shows nearly constant ratios L for simultaneous loads,  $L=M_y/F_x$  and  $L=M_x/F_y$ . This ratio L is the lever arm

where  $F_{xz}$  and  $F_{yz}$  should be applied.



The blade root loadings  $F_x$ ,  $F_y$ ,  $M_x$ ,  $M_y$  are according to the GL-coordinate (Germanischer Lloyd) system in fig 2.

fig 2 blade coordinate system according to GL

There is also a nearly constant ratio  $C=M_y/M_x$ , as shown in fig 6. So the loads for one rotor blade can be applied with one actuator located in a distance  $L$  and in a certain direction  $\alpha_z$  according to fig 3.

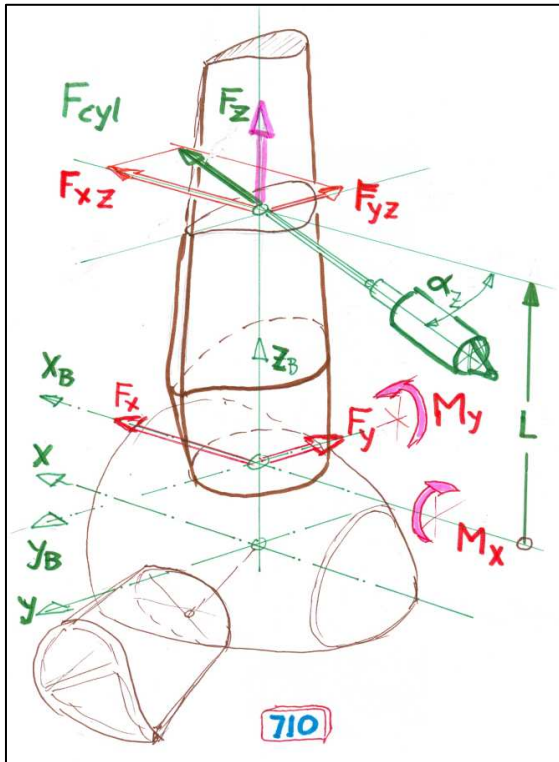


fig 3 one force  $F_{cyl}$  on one blade

Again the main bending moment  $M_x$  at the blade root comes from dead weight of the blade and can be simulated by rotating mass  $m$  without extra power consumption.

The other feature of this concept is to separate the high frequency inputs into low frequency loads with high amplitudes and into high frequency loads with very small amplitudes. Both categories of the load will be applied by different mechanisms. Low frequency loading is to be applied by electric or hydraulic actuators using RPC techniques. In a real turbine these loadings are coming from low frequency changes in wind direction and velocity. Wind turbulences are causing high frequency responses and should be reproduced by random loads from rotating masses at low energy input.

Our new concept exploits both of these features and simplifies the testing rig in comparison to existing wind turbine testing equipment. In the following we will explain these features in more detail.

**3. One force at one distance L for all blade root bending loadings**

Analysing simultaneous loads  $M_y$  and  $F_x$  in a time history shows results according to fig 4. There is always a constant ratio  $L_1$  between  $M_y$  and  $F_x$  at the blade root. In fig 4 12000 data for load points  $M_y$

versus  $F_x$  at the blade root are presented. These data are the output of a load simulation with Bladed code from Garrad Hassan run for 10 minutes for power production at 10 m/s wind speed.

About the same results would be obtained from measurements on a 2.5 MW wind turbine. Nearly the same ratio  $L_2$  would be seen between  $M_x$  and  $F_y$ .

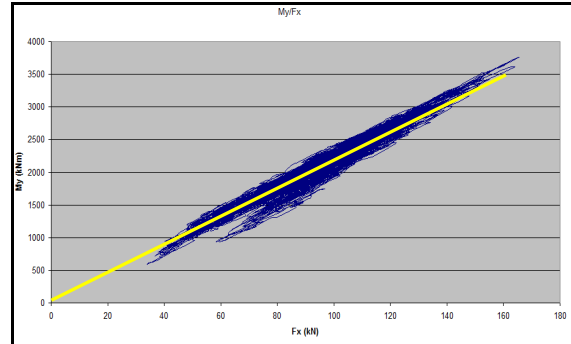


fig 4 12000 data  $M_y$  versus  $F_x$

It is another important feature of this concept to use the same lever arm  $L = L_1 = L_2$  as distance for the load input  $F_{xz}$  and  $F_{yz}$ . These data are close to a yellow line, that is an acceptable approach for the arm  $L_1$  on the blade, a desired shear force  $F_x$  and the desired bending moment  $M_y = F_x * L_1$  will be generated at the blade root. The same applies also for the ratio  $L_2 = M_x / F_y$ , that is nearly the same as  $L_1$ .

The wind speed  $w$  and the circumferential velocity  $u$  of the turbine create a resultant velocity  $c$ , that forms an angle  $\alpha$ , called the angle of attack, with the chord line of the blade. See fig 5.

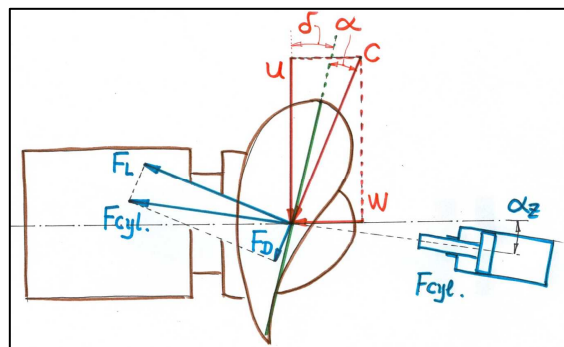


fig 5 speeds and forces on the blade segment

As known from aerodynamics the resultant velocity  $c$  creates two forces on the blade segment: one is lifting force  $F_L$  vertical to the velocity  $c$ , the other one is drag force  $F_D$  along the velocity  $c$ . These two forces form a resultant force  $F_{cyl}$ , that can be divided into  $F_{xz}$  in wind direction and  $F_{yz}$  in rotor rotating direction.  $F_{xz}$  and  $F_{yz}$  cause as already explained  $F_x$ ,  $M_y$  and  $F_y$ ,  $M_x$  at the blade root, where  $F_{xz}$  and  $F_{yz}$  represent the load summary from all blade elements along the blade. See fig 3

Analysing time histories of simultaneous bending moments  $M_y$  and  $M_x$  at the blade root, shows a ratio  $C=M_y/M_x$  in an area between 6.7 and 13.6. See fig 6. It will be explained later how  $M_y$  and  $M_x$  as responses at the blade root are created.

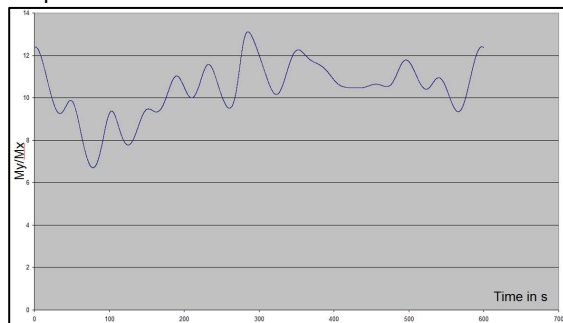


fig 6 ratio C between  $M_y$  and  $M_x$

The ratio C depends on  $\alpha_z$  that can be calculated from the formula

$$\alpha_z = \text{arccot}(M_y/M_x)$$

resulting in values between  $\alpha_{z\text{max}} = 8.48^\circ$  and  $\alpha_{z\text{min}} = 4.2^\circ$ . As a practical result the components  $F_{xz}$ ,  $F_{yz}$  at the load input point L can be reproduced by actuator load  $F_{Cyl}$  and the appropriate angle  $\alpha_z$ . Each actuator input will produce dynamic responses at the blade root:  $F_x$ ,  $F_y$ ,  $M_x$ ,  $M_y$ . Control procedures like RPC (remote parameter control) by MTS systems corporation are needed.

#### 4. Load Separation by frequencies

As mentioned in the summary equipment for wind turbine drive train have a very large energy consumption up to 200% of the rated turbine power. This is because high frequency wind loads are reproduced by high speed hydraulic actuators. In addition the size of the drive motor has double the rated torque of the gear box in order to provide the high frequency torque input.

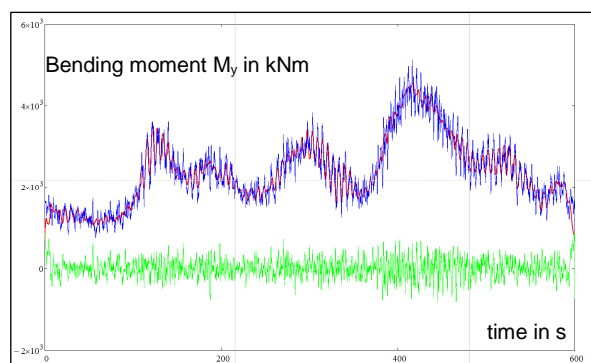


fig 7 bending  $M_y$  at the blade root at 6 m/s wind speed

The fig 7 shows measured or simulated data for  $M_y$  during power production at 6 m/s wind speed using Bladed code in blue colour.

By the use of Fourier analysis (FFT) loads with high frequencies can be separated into two parts: low frequency loads  $M_{yLF}$  in red colour and high

frequency loads  $M_{yHF}$  with very small amplitudes in green colour.

Fig 8 is a detail from 0 to 100 seconds on the time scale of fig 7.

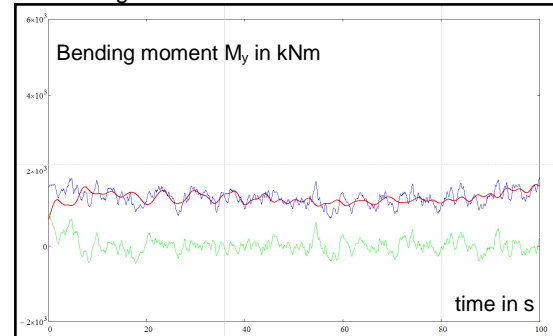


fig 8 detail from 0 to 100 s

The low frequency signals will be simulated by the actuators and the high frequency signals by random loads from rotating masses.

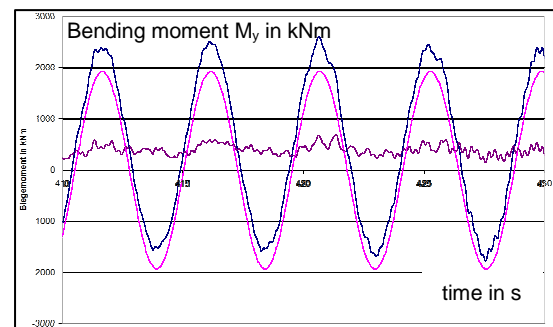


fig 9 bending  $M_x$  at the blade root at 6 m/s wind speed

Fig 9 presents measured or simulated data for  $M_x$  from the same power production time frame (as blue line).

The main component  $M_{xdw}$  of  $M_x$  at the blade root is caused automatically by the dead weight of the blade itself and can be generated by a mass at the end of the blade dummy. The difference (in brown colour) will also be FFT analysed to create a low frequency signal to be used as desired response in the control loop. The high frequency signals will also be generated by random loads from rotating masses.

#### 5. Testing rig configuration

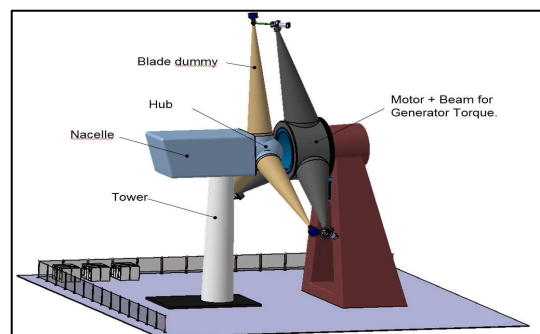


fig 10 testing rig configuration

In fig 10 the testing rig configuration is presented. The drive motor, that provides the torque for the test turbine is shown on the right and the turbine itself on the left side. In fig 11 details of the load input actuator are shown.

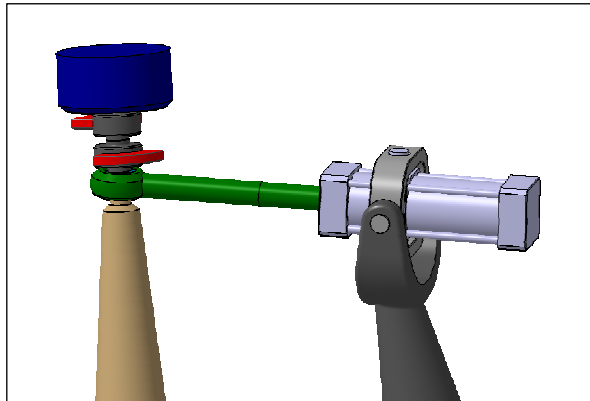


fig 11 details for the load introduction mechanism

Each actuator is for introduction loads  $F_{Cyl}$  (200 to 430 kN) by using displacement reference signals  $s_z$ , so that bending moments  $M_x$  and  $M_y$  as responses with low frequencies at the blade root are simulated.

The mass  $m=10$  t (in blue colour) generates together with the blade dummy  $m=3$  t the bending moment from dead weight  $M_{xdw}$  at the blade root automatically.

Two rotating exciters in red colour (each having a mass of 2 kg and eccentricity of 100 mm) are for introduction of random forces with high frequencies, so that also bending moments  $M_x$  and  $M_y$  with high frequency content are simulated.

Together with desired bending moments  $M_x$  and  $M_y$ , the shear forces  $F_x$  and  $F_y$  will be introduced at the blade root at the same time. (See fig 3)

### 6. Multi body Simulation for the Test System

A multi body simulation code was used to create and understand the dynamic load transfer between the test rig model and the turbine drive train model with a flexible rotor (see fig 12).

The turbine hub was operated with a constant speed  $n$  at the hub. Three flexible blade dummies with one fixed and two rotating small masses produced input loads at a distance  $L$  from the blade bearing surface on the hub. The responses were recorded as blade bending moment  $M_x$  and  $M_y$  on each blade root.

Fig 13 shows bending moment  $M_y$  with a low frequency content mainly from the dead weight of the mass  $m$  and a high frequency vibration caused by random load input from rotating masses. It is assumed, that any desired low frequency bending moment  $M_y$  and  $M_x$  can be obtained by using Remote Parameter Control techniques (RPC) to create the input reference values for the

displacement  $s_z$  of the three actuators, the motor torque at the speed  $n$  which is identical to the hub speed. In addition the angle  $\alpha_z$  between the angular position of the hub and the drive motor is a further input.

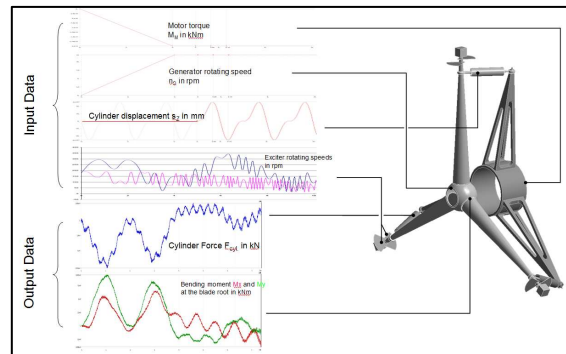


fig 12 inputs and outputs for multi body simulation

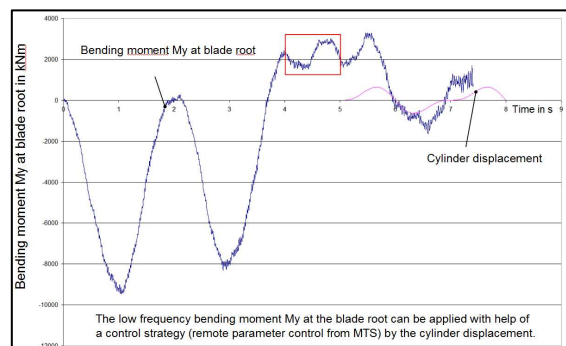


fig 13  $M_y$  at the blade root from testing rig simulation

### 7. Remote Parameter Control Procedure

There are control procedures available that are able to operate test rigs for automotive cars or other dynamic systems with multiple input and remote responses.

Fig 14 illustrates the procedure for system identification. White noise or other known signals

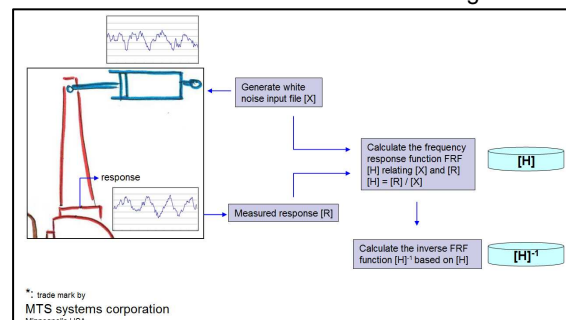


fig 14 system identification

are used as input signals like voltage for servo valves on hydraulic actuators. The response signals like bending stress or acceleration on remote sensors are measured and the frequency transfer functions  $[H]$  from each input to each response are calculated and stored on a disc.

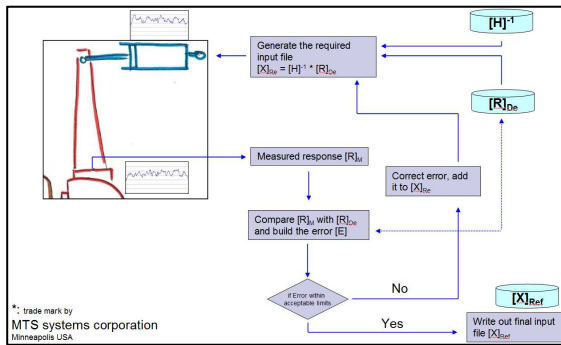


fig 15 final required reference input calculation

In fig 15 the procedure for obtaining final required reference input signals is illustrated.

In a first step the required input  $[X]_{Re}$  is calculated from the desired response  $[R]_{De}$  and the inverse frequency transfer function  $[H]^{-1}$ .

Using this input creates response signals  $[Re]$  on the sensors that are compared with the desired responses  $[Re]_{De}$ . The error is used to correct the input in several iteration steps until the responses are close to the required ones and the final reference input file is stored.

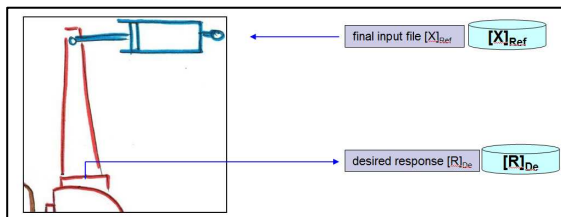


fig 16 run the testing rig with final required reference inputs

In fig 16 the final input file  $[X]_{Ref}$  is used to perform the test by reproducing loads for several design load cases and repeating according to their occurrence in the turbine life time.

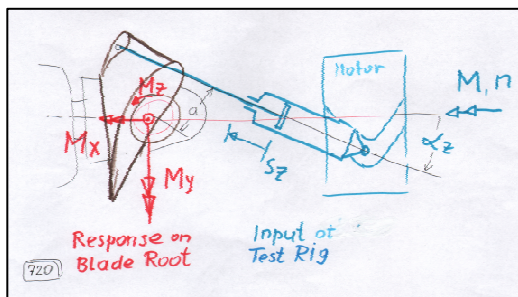


fig 17 inputs and outputs on the testing rig

In fig 17 blade root bending moments  $M_y$  and  $M_x$  on each blade are the desired response signals  $[Re]_{De}$  as they have been measured in a real wind turbine or they have been calculated in the load simulation model like Bladed code from GH. The required input reference  $[X]_{Ref}$  signals for the test rig are the actuator displacements  $S_{z1,2,3}$ , the motor torque  $M$  and the motor speed  $n$ . The flexible blade dummy leads to the distance  $a$  between blade root centre

and the loading point for the actuator. Therefore the torsional moment  $M_z$  will be created automatically.

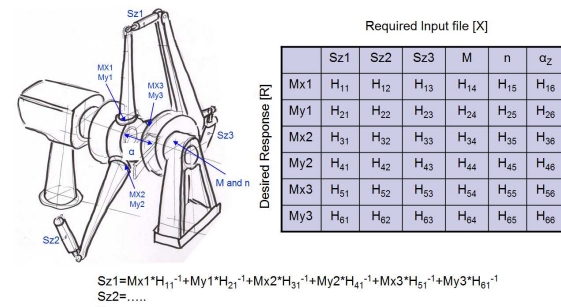


fig 18 transfer functions [H]

Fig 18 presents the frequency transfer functions  $[H]$ , and the procedure to calculate the input reference signals  $S_{z1}$ .

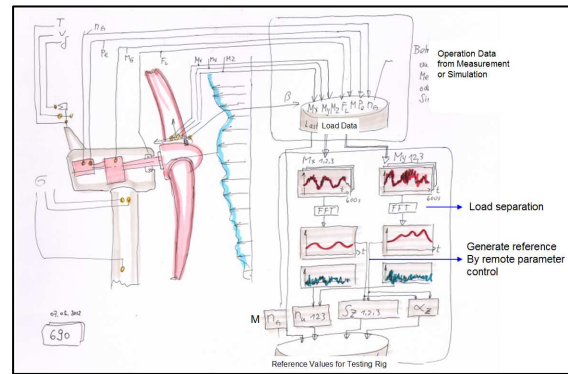


fig 19 all required input data for the testing rig

Fig 19 shows data from an operating turbine to be stored. Low and high frequency bending moments are separated and RPC procedures are used to acquire the input for the test rig (fig 1).

### 8. Conclusion

The proposal is for wind turbine fatigue testing, where high frequency loading can be applied to the rotor blade bearings in order to simulate 18 load components on three blades with only three actuators. The largest loading on the hub of Multi Megawatt Turbines is coming from the dead weight of the blades. By using rotating masses, this loading is simulated with no extra power needs.

High frequency vibration wind turbulences are applied by random loads from rotating masses. The relationship between random loads and their rotary speed has to be defined in more detail for this application.

#### Reference

Udayan N. Godbole, Master thesis an MTS Institute: Vehicle Road Test Simulation